Supplementary Information

Transient tap couplers for wafer-level photonic testing based on optical phase change materials

Yifei Zhang[1,*], Qihang Zhang[1], Carlos Ríos[1], Mikhail Y. Shalaginov[1], Jeffrey B. Chou[2], Christopher Roberts[2], Paul Miller[2], Paul Robinson[2], Vladimir Liberman[2], Myungkoo Kang[3], Kathleen A. Richardson[3], Tian Gu[1], Steven A. Vitale[2], Juejun Hu[1,*]

[1]Department of Materials Science and Engineering, Massachusetts Institute of Technology, Cambridge, 02139, Massachusetts, USA

[2]Lincoln Laboratory, Massachusetts Institute of Technology, Lexington, 02421, Massachusetts, USA

[3]College of Optics and Photonics, University of Central Florida, Orlando, 32816, Florida, USA

*yzhang94@mit.edu, hujuejun@mit.edu

7 pages, 3 figures, 3 tables

This Supplementary Information comprises the following Sections:

I. Optical constants of GSST.

II. Transient tap coupler in a SiN photonic platform.

III. Tolerance study of the transient tap coupler.

Section I – Optical constants of GSST.

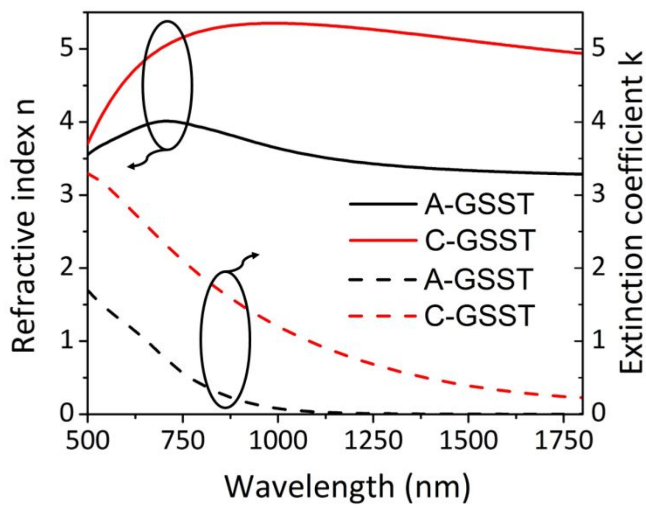

Fig. S1. Optical constants of amorphous (black lines) and crystalline (red lines) phases of $Ge_2Sb_2Se_4Te_1$ from the visible range to near-infrared. The solid lines represent the refractive index n, and the dashed lines represent the extinction coefficient k.

The O-PCM implemented in this invention, Ge-Sb-Se-Te or GSST, is derived from the conventional GST alloy by partially substituting Te with Se[1]. Figure S1 shows the optical constants of GSST, which were measured using ellipsometry on thermally evaporated films. Specifically, optical attenuation in a-GSST is vanishingly small in the telecom window, well below the sensitivity limit of ellipsometry. We therefore opted for a waveguide cut-back method to quantify the loss in a-GSST[2], which yields an extinction coefficient $k = (1.8 \pm 1.2) \times 10^{-4}$—over 1000 times smaller than that of GST. In its crystalline phase, c-GSST yields a moderate extinction coefficient of 0.39 at 1550 nm. Although it is much lower than that of c-GST, it is still prohibitively high for guided-wave devices. Hence, directing the light away from the lossy crystalline c-GSST via index mismatching is essential for obtaining a minimal insertion loss in our tap coupler device.

Section II – Transient tap coupler in a SiN photonic platform

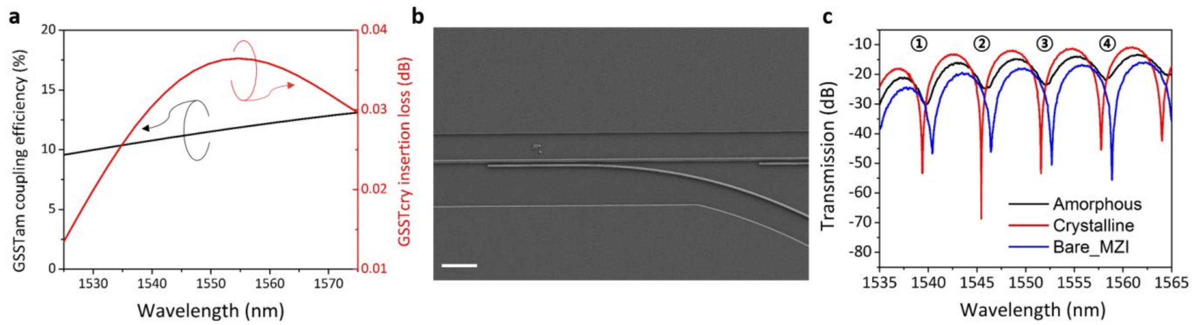

Fig. S2. (a) Simulated coupling efficiency in the amorphous state (black line) and insertion loss in the crystalline state (red line) for a SiN tap coupler. (b) SEM image of the fabricated transient tap couplers cascaded on the SiN main waveguide; scale bar 10 µm. (c) Measured transmission spectra of bare MZI device (blue), MZI with amorphous (black) and crystalline (red) tap couplers in the shorter arm.

The proposed tap coupler design is not tied to a particular material platform. To demonstrate the cross-platform capability of this design, we also demonstrate a transient tap coupler on a SiN platform. The geometry of the optimized design is: h = 400 nm, h_p = 40 nm, w_g = 620 nm, w_m = 780 nm, w_t = 600 nm, w_p = 450 nm. As shown in Fig. S2 (a), when the total coupling length of the device is 24 µm, the simulated coupling efficiency is around 11.5% at amorphous state, and the insertion loss is around 0.036 dB (0.82%).

In order to measure the insertion loss at crystalline state, an unbalanced Mach–Zehnder interferometer (MZI) is used. Six tap couplers are cascaded onto the shorter arm of the MZI, and insertion loss can be inferred from the extinction ratio (ER) of the transmission spectra of the MZI devices[3].

Table S1. Extinction ratios of the MZI interference at different wavelength point.

Extinction ratio	Wavelength point ①	Wavelength point ②	Wavelength point ③	Wavelength point ④
Bare MZI	24.5	27	32.5	39
Amorphous	11.5	9	8.9	8.2
Crystalline	37	55	41	34

In table S1, we list the ERs of the MZI spectra at different wavelength point. Since ERs vary quite a lot at different wavelength points even within the same spectrum, we need to calculate the IL and coupling efficiency at each wavelength point. We notice that ER for bare MZI increases linearly with wavelength, whereas it first increase then decrease for MZI with crystalline taps on its shorter arm. Therefore we conclude that for wavelength point ①, the loss induced by the insertion loss of crystalline tap couplers does not compensate the loss difference between the two arms, whereas for wavelength point ③ and ④, the loss induced by crystalline tap couplers surpasses the loss difference between the two arms. For wavelength point ②, we treat it the same way as wavelength point ③ and ④ in order to get the upper bound of insertion loss.

The unbalanced arm lengths in the MZI devices account for the fringes in the transmission spectra. Assume the amplitude ratio between the longer arm and the shorter arm is A (0<A<1 due to higher loss in the longer arm), then the extinction ratio of the MZI, i.e., the ratio of the maximum transmission over the minimum transmission, can be expressed as:

$$ER_1 = \frac{T_{max}}{T_{min}} = \frac{|1+A|^2}{|1-A|^2}$$

where ER_1 denotes the extinction ratio for the bare MZI. Similarly, assume the amplitude in the shorter arm decreases to B (0<B<1) when the crystalline tap couplers are present, then the new extinction ratio can be expressed as:

$$ER_2 = \frac{T_{max}}{T_{min}} = \frac{|B+A|^2}{|B-A|^2}$$

where ER_2 denotes the extinction ratio for the MZI with crystalline tap couplers on its shorter arm. When the loss induced by the insertion loss of crystalline tap couplers exceeds the loss difference between the two arms, i.e., B<A, B can be calculated by:

$$B = \frac{\sqrt{ER_2}-1}{\sqrt{ER_2}+1} \times \frac{\sqrt{ER_1}-1}{\sqrt{ER_1}+1}$$

When the loss induced by the insertion loss of crystalline tap couplers does not compensate the loss difference between the two arms, i.e., B>A, B can be calculated by:

$$B = \frac{\sqrt{ER_2}+1}{\sqrt{ER_2}-1} \times \frac{\sqrt{ER_1}-1}{\sqrt{ER_1}+1}$$

In both cases, the coupling strength of a single tap coupler can be inferred from B as:

$$Coupling\ strength = 1 - B^{2/n}$$

where n is the number of tap couplers.

Table S2. Coupling efficiency and insertion loss at different wavelength point.

	Wavelength point ①	Wavelength point ②	Wavelength point ③	Wavelength point ④
Coupling efficiency	19.9%	24.2%	23.4%	24.5%
Insertion loss	3.0% (0.13 dB)	3.0% (0.13 dB)	2.2% (0.095 dB)	2.1% (0.09 dB)
Contrast ratio	6.6	8.1	10.6	11.7

In table S2, we summarize the tap coupler performance at the four wavelength points. The obtained coupling efficiency and insertion loss are relatively consistent at those wavelengths. We note that the coupling efficiency and insertion loss are both significantly higher than the simulation results. We attribute this discrepancy to the possible systematic fabrication error, such as waveguide width, refractive index of SiN and thickness of SiN – in the case when such fabrication error causes a smaller light confinement in the fabricated waveguides than that in simulation, light coupling between the waveguides will be enhanced. We note that this discrepancy can be overcome in the industrial setting when the fabrication processes are standardized.

We also note that two different methods are adopted for measuring the SOI and SiN tap couplers. It is because for SOI tap couplers, the insertion loss is too low to be measured accurately with unbalanced MZI method.

The uncertainty of the unbalanced MZI method mainly comes from two parts. Firstly, the dynamic range of the setup determines the minimal loss difference we are able to detect between two arms of the MZI. Our setup has a noise level down to -85 dB, which in our case is well below the interference dips in the spectra. Secondly, the uncertainty in the ER plays a more important role. We notice that the loss difference between two arms has a wavelength dependence in the bare MZI spectrum. Since the interference dip does not happen at the exact same wavelength for bare MZI and MZI with crystalline tap couplers, we estimate there can be a 0.5 dB uncertainty in the ER of the bare MZI, for wavelength point ② for example. This translates to an error of ~0.01 dB for the 0.13 dB/coupler result.

On the other hand, for the cutback method, our experiments are performed with a grating coupler setup, and the transmission response was maximized by optimizing the position of the input and output fibers. We have characterized the system by measuring identical waveguide devices multiple times to quantify the variation of coupling losses due to the gratings and misalignment, and concluded that the systematic error of this measurement method is within 5%, which translates to an error of ~0.0026 dB for the 0.01 dB/coupler result.

We summarize the relative strengths and weakness of the two approaches in table S3.

Table S3. Comparing the cutback method and the unbalanced MZI method.

Measurement method	Cutback method	Unbalanced MZI method
Strength	Able to measure low ILs	Not subject to systematic alignment error of the grating coupler setup
Weakness	Subject to systematic error of the grating coupler setup. The error however decreases as the number of the stringed devices under test increases, which applies to low-loss SOI devices.	Unable to measure low ILs

Section III – Tolerance study of the transient tap coupler.

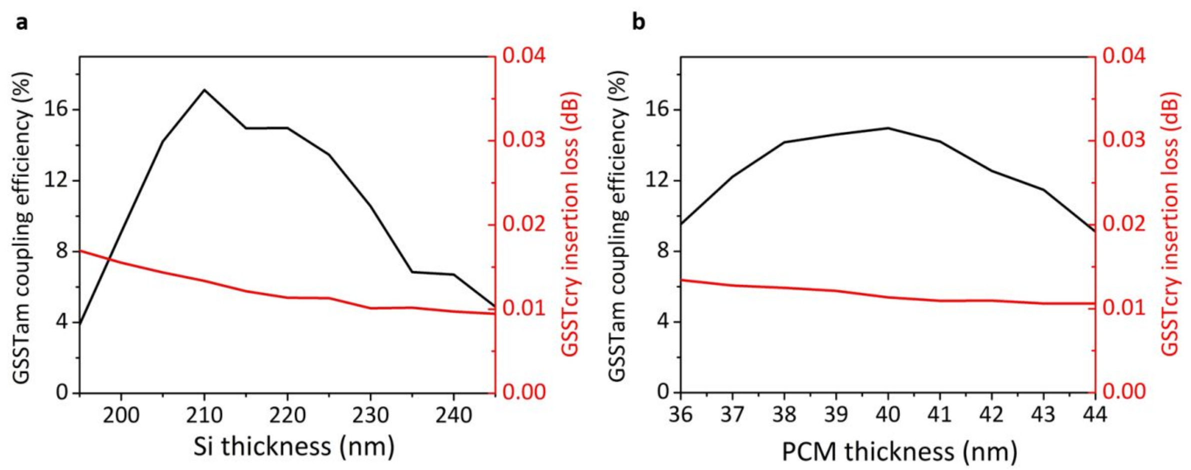

Fig. S3. Tap coupler performance as a function of (a) silicon layer thickness and (b) PCM thickness.

The main sources of cross-wafer variations have been shown to originate from thickness changes of the SOI layer, which can be up to 10% across a 200 mm wafer[4]. In addition, PCM film thickness variations across a wafer may also contribute to the variation. We have therefore performed tolerance studies investigating both sources of variations, considering up to 10% thickness changes. The results at 1550 nm are summarized in Fig. S3.

The result shows that the IL remains below 0.02 dB, and coupling efficiency is above 6% for a thickness variation of ± 20 nm for the silicon layer and above 8% for a thickness variation of ± 4 nm for the PCM layer, which is adequate for wafer-scale photonic testing. We can also further increase the coupling length to increase the coupling efficiency without sacrificing the IL considerably.

References

(1) Zhang, Y.; Chou, J. B.; Li, J.; Li, H.; Du, Q.; Yadav, A.; Zhou, S.; Shalaginov, M. Y.; Fang, Z.; Zhong, H.; Roberts, C.; Robinson, P.; Bohlin, B.; Ríos, C.; Lin, H.; Kang, M.; Gu, T.; Warner, J.; Liberman, V.; Richardson, K.; Hu, J. Broadband Transparent Optical Phase Change Materials for High-Performance Nonvolatile Photonics. *Nat. Commun.* **2019**, *10* (1), 4279. https://doi.org/10.1038/s41467-019-12196-4.

(2) Zhang, Q.; Zhang, Y.; Li, J.; Soref, R.; Gu, T.; Hu, J. Broadband Nonvolatile Photonic Switching Based on Optical Phase Change Materials: Beyond the Classical Figure-of-Merit. *Opt. Lett.* **2018**, *43* (1), 94. https://doi.org/10.1364/ol.43.000094.

(3) Lin, H.; Song, Y.; Huang, Y.; Kita, D.; Deckoff-Jones, S.; Wang, K.; Li, L.; Li, J.; Zheng, H.; Luo, Z.; others. Chalcogenide Glass-on-Graphene Photonics. *Nat. Photonics* **2017**, *11* (12), 798.

(4) Selvaraja, S. K.; Rosseel, E.; Fernandez, L.; Tabat, M.; Bogaerts, W.; Hautala, J.; Absil, P. SOI Thickness Uniformity Improvement Using Corrective Etching for Silicon Nano-Photonic Device. *IEEE Int. Conf. Gr. IV Photonics GFP* **2011**, 71–73. https://doi.org/10.1109/GROUP4.2011.6053719.